# A GENERAL APPROACH TO THE MEASUREMENT OF THERMAL RESIDUAL STRAINS AND STRESSES IN SiCw/Al COMPOSITES

Q. Y. Liu[1,2] W. D. Fei[2]
[1] *LNM, Institute of Mechanics, Chinese Academy of Sciences, Beijing 100080, P. R. China*
[2] *School of materials science and engineering, Harbin Institute of Technology, Harbin 150001, P. R. China*

**SUMMARY:** On changing temperature, traditional macrostress and microstress as well as thermal mismatch stress will exist in SiCw/Al composites, thermal mismatch stress was emphasized on in this paper. Firstly, thermal mismatch stresses-strains in a single SiC whisker were analyzed; and then effects of thermal mismatch stress on the position of X-ray diffraction peak were discussed, the relationship between thermal residual strains and the shift of diffraction peak was established. On the basis of the above discussion, considered the special crystallographic characteristics of β-SiC whisker, a new measurement method of thermal mismatch stress was developed by measuring the lattice distortion of SiC whisker. Thermal mismatch stresses in SiCw/Al composites were calculated, and the results agreed well with the previous research works.

**KEYWORDS:** SiCw/Al composites, thermal residual strains and stresses, X-ray diffraction

## INTRODUCTION

It was well recognized that thermal residual stresses could be introduced into metal matrix composites (MMCs) when MMCs were cooled down to room temperature from fabrication or quench temperature[1,2,3]. Thermal residual stresses were inherent characteristics of SiCw/Al composites due to the difference of thermal expansion coefficient (CET) between silicon carbide whisker and aluminium alloy ( the CET of SiC whisker is $4.7*10^{-6}$/K and Al is $23.6*10^{-6}$/K). Many properties of composites, such as yield stress, creep rate, fatigue lifetime as well as dimensional stability, can be influenced by thermal residual stresses, for example, a higher compression yield stress than tensile yield stress can be obtained in SiCw/Al composite.

Thermal residual stresses attracted more attention recently, it was very difficult to eliminate thermal residual stresses completely by means of heat treatment. Main research works focused on the following two aspects: firstly, the formation mechanisms and the distribution characteristic of thermal residual stresses were analysed using the theory model including Eshelby method or finite element model[4-7]; Secondly, stresses (strain) measurement and the effects of thermal residual stresses on the properties (such as Bauschinger effects and deformation behavior ) were investigated[8,9]. For mathematical simplicity, whisker aligned was assumed when Eshelby model or finite element model were used to study thermal residual stresses in composites reinforced by whisker. Little work has been done to investigate thermal residual stress in the composite in which the whisker distributed randomly. The aim of this paper was to introduce a new method suitable to measure thermal residual stresses in randomly oriented composite.

## EXPERIMENTAL

The reinforcement used was β-SiC whisker with face center cubic structure obtained from Tokai Carbon Co. Ltd of Japan. The matrix was commercial 6061 aluminium alloy. The SiCw/Al composite with whisker volume fraction of 20% was fabricated by squeeze-casting method. The dimension of the specimen for X-ray diffraction was ϕ5 mm× 0.5 mm. The specimens were solution-treated at 520¡æfor 2h, then quenched into water.
The θ-2θ co-rotation method was employed in X-ray diffraction test using $CuK\alpha_1$ radiation to measure thermal residual strain with the tube voltage of 50KV and current of 25 mA. Step scan method with the step of 0.02° was used.

## MEASURED METHOD OF THERMAL MISMATCH STRESS

### Thermal residual stresses in SiCw/Al composites

Firstly, thermal residual stresses in the specimens of SiCw/Al composites were analysed. On changing temperature, traditional macrostress and microstress as well as thermal mismatch stress (formed due to the difference of thermal expansion coefficient between SiC whisker and Al alloy ) will form in composites. The specimens used in this experiment were so thin (less than 0.5mm) that macrostress can be neglected. It was well known that microstress can only causes the widening of X-ray diffraction peak because microstress was self-equilibrate in the grain, and they had no influence on the shift of X-ray diffraction peak[10] . Therefore, the shift of X-ray diffraction peak in SiCw/Al composites only caused by thermal mismatch stress, which was emphasised on in this paper. A new experiment method was developed to measure thermal mismatch stress by measuring the lattice distortion of SiC whisker in SiCw/Al composites in which whisker distributed randomly.
The volume average of thermal mismatch stress between reinforcement and matrix in SiCw/Al composites were zero (thermal mismatch stress was self-equilibrated internal stress for it was free from any other external force and surface constraint.), the intrinsic phase average of thermal mismatch stress in matrix and reinforcement were unlike signed and nonzero, which can cause the opposite shift of X-ray diffraction peak. Therefore, if the intrinsic phase average of thermal mismatch stress in matrix or reinforcement can be known, according to stresses equilibrium equation, the intrinsic phase average of thermal mismatch stress in the other phase can be deduced. SiC whisker with higher melting point and strength can keep completely elastic state during heat-treatment procedures, the position of X-ray diffraction peak of SiC whisker only changed with the changing of thermal mismatch stress in them, so it was easy to measure thermal mismatch strain (and stress) in SiCw/Al composite by measuring the shift of X-ray diffraction peak of SiC whisker.

### Basic assumptions

For the sake of simplicity, to take the following assumptions were necessary :
1. Whiskers distribute randomly and uniformly in the matrix within the radiation volume of X-ray. It was no double that whiskers distributed randomly and uniformly in the matrix for SiCw/Al composites fabricated by squeeze casting technique. Meanwhile, the radiation volume of X-ray contained a lot of whiskers, based on this fact, assumption 1 was reasonable. Therefore, X-ray measurement results of the samples were dependent mainly on their heat-treatment procedures but not related to what modes were employed to set the samples on the test shelf.

2. A single whisker in the composite was randomly singled out and a local column coordinate system was established, as illustrated in Fig.1, assuming that thermal mismatch stress was the same for all whiskers within the radiation volume of X-ray, which was denoted as $\sigma_{ij}$. At the same time, assuming that thermal mismatch stress was also the same in different zones in a certain single whisker.

It was worth noting that the stress states in different zones in a certain single whisker and for different whiskers in the practically fabricated composites were somewhat different. For all that, the second assumption was well supported by the following two points. First of all, as mentioned above, random and uniform distribution of whiskers in the matrix leaded the composites macroscopically isotropical. So it can be thought that X-ray measurement results will not be affected by the setting of the samples. That was to say, the fluctuation of the stress in different oriented whiskers in the composites will not exert an influence on the X-ray measurement results. Furthermore, the average values of variation of crystal-plane distance of whiskers producing diffraction will be measured by means of X-ray diffraction within the detectable volume. Fluctuation of stress in different whiskers and different zones in the same single whisker mainly contributed to widening of diffraction peak and had no effect on displacement of diffraction peak, therefore, it was reasonable to neglect the effect of fluctuation of stress. In a word, as far as all whiskers producing diffraction were concerned, residual thermal mismatch stress were the same, which have nothing to do with a certain single whisker and locations in the same single whisker.

3. Distribution of stresses in whiskers was axially-symmetric.

For a single whisker with a large aspect ratio of about 20~50 and a very small diameter of about 0.5~1.0μm, based on the second assumption, it was well thought that distribution of stress in whiskers was axially symmetric. Nonzero stress components were $\sigma_r$, $\sigma_\theta$ and $\sigma_z$, and $\sigma_r$ equalled to $\sigma_\theta$. Radial and longitudinal stresses and strains in the whisker were denoted as $\sigma_r$, $\varepsilon_r$ and $\sigma_z$, $\varepsilon_z$, respectively, as shown in Fig.1.

**Thermal mismatch strain-stress in SiC whisker**

According to the second assumption, the strains of different zones in the same whisker were considered the same, namely, $\varepsilon_r = \varepsilon_\theta$, stress and strain in the whisker had the following relationship:

$$\left.\begin{aligned}\sigma_r &= \lambda e + 2\mu\varepsilon_r \\ \sigma_z &= \lambda e + 2\mu\varepsilon_z\end{aligned}\right\} \qquad £¨1£©$$

in which $e = \varepsilon_r + \varepsilon_z + \varepsilon_\theta = \varepsilon_z + 2\varepsilon_r$ represented volume strain, λ and μ were Lame constants of the SiC whisker, $\sigma_r$ and $\sigma_z$ were radial and longitudinal thermal mismatch stress, respectively. From the above relationship formula, if radial and longitudinal residual strains ($\varepsilon_r$ and $\varepsilon_z$) can be measured out, radial and longitudinal residual thermal mismatch stresses will easily be obtained.

According to assumption 1, it was followed that macroscopic stress of the reinforcement (also volume average stress ) was a spherical symmetry tensor, so:

$$\langle \boldsymbol{\sigma} \rangle_w = \begin{pmatrix} \sigma_w^0 & 0 & 0 \\ 0 & \sigma_w^0 & 0 \\ 0 & 0 & \sigma_w^0 \end{pmatrix} \qquad £¨2£©$$

In the macroscopic coordinate system labelled 1, 2, 3 in Fig.2, $\langle \sigma_{33} \rangle_w = \sigma_w^0$. Meanwhile, for the whiskers which longitudinal axial direction was at an angle of ϕ to Axis 3, $\sigma_{33} = \sigma_z \cos^2 \phi + \sigma_r \sin^2 \phi$. The second assumption suggested that stress in every whisker was the same, hence:

$$\sigma_w^0 = \langle \sigma_{33} \rangle_w = \frac{1}{4\pi} \iint \sigma_{33} d\Omega$$
$$= \frac{1}{4\pi} \int_0^{2\pi} \int_0^{\pi} \sigma_{33} \sin\phi d\phi d\theta = \frac{1}{3}\sigma_z + \frac{2}{3}\sigma_r \qquad £¨3£©$$

Obviously, if all stress components were known, the intrinsic phase average thermal mismatch stress in the whisker was easily obtainable. Furthermore, according to the balance rule of thermal mismatch stress, intrinsic phase average thermal mismatch stress in the matrix was also obtained in terms of the following equation:

$$V_f < \boldsymbol{\sigma} >_w + (1 - V_f) < \boldsymbol{\sigma} >_m = 0 \qquad £¨4£©$$

where $V_f$ was the volume fraction of whiskers, $< \boldsymbol{\sigma} >_w$ and $< \boldsymbol{\sigma} >_m$ were intrinsic phase average thermal mismatch stresses in the whisker and the matrix, respectively. Since $< \boldsymbol{\sigma} >_w$ was a spherical symmetry tensor, $< \boldsymbol{\sigma} >_m$ was also a spherical symmetry tensor, so:

$$\langle \boldsymbol{\sigma} \rangle_m = \begin{pmatrix} \sigma_m^0 & 0 & 0 \\ 0 & \sigma_m^0 & 0 \\ 0 & 0 & \sigma_m^0 \end{pmatrix} \qquad £¨5£©$$

Therefore, Eqn.(4) can be rewritten as the following£º

$$V_f \sigma_w^0 + (1 - V_f)\sigma_m^0 = 0 \qquad £¨6£©$$

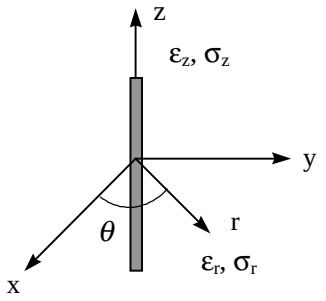


Fig.1 Diagram of local column coordinate system in SiC whisker

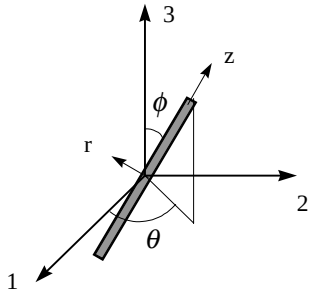


Fig.2 Diagram of orientation of SiC whisker in the macroscopic coordinate system

**Dependence of diffraction peak displacement on residual strains in SiC whisker**

The growth direction of β-SiC whiskers with a fcc structure from all manufactures was <111> direction (longitudinal axis) which has been well substantiated by previous research[11], as indicated in Fig.3. Just on account of the special crystallographic characteristics of the SiC whisker, to measure elastic strain components in the whisker became possible. For analysis simplicity, it was assumed that longitudinal axis of the whisker was [111]z (corresponding crystal plane denoted as $(111)_z$ ), and the other <111> being at an angle of $\phi_1$ ($\phi_1$ =±cos$^{-1}$(1/3)) to the longitudinal axis direction were denoted as $[111]_{\phi 1}$, (also corresponding crystal plane

denoted as $(111)_{\phi 1}$ ), as shown in Fig.3-a. As for the randomly oriented composites, on measuring the diffraction peak in any direction, probability of all crystal planes producing diffraction does not equal zero. So it was necessary to present the relationship between diffraction peak displacement and all strain components in the whisker.

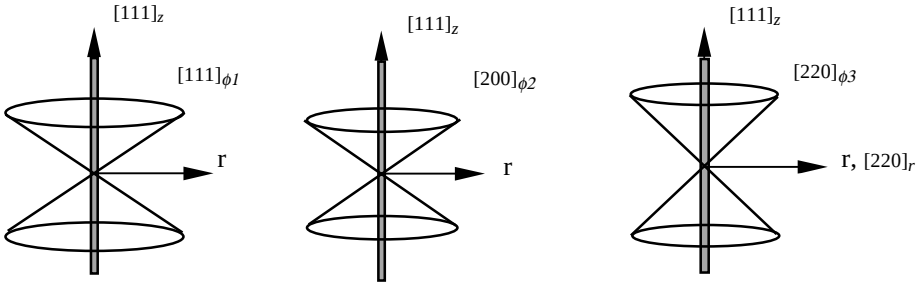


(a) (b) (c)

Fig.3 Distributions of crystalline direction of β-SiC whisker corresponding to the longitudinal direction of SiC whisker, (a)<111>, (b)<200>, (c)<220>

It was reasonably thought that 111 diffraction can be attributed to the combined diffraction of two groups of crystal planes, $(111)_z$ and $(111)_{\phi 1}$ in the SiC whisker. Diffraction integrity strength and normalised peak shape function of $(111)_z$, $(111)_{\phi 1}$ were denoted as $I_{111z}$£¬$G_{111z}$ and $I_{111\phi 1}$£¬$G_{111\phi 1}$£¬respectively. According to Rietveld[18] theory of overall spectrum simulation, 111 diffraction line strength of SiC whisker complied with the following formula:

$$I_{111}(\theta) = I_{111z} \cdot G_{111z}(\theta - \theta_{111z}) + I_{111\phi 1} \cdot G_{111\phi 1}(\theta - \theta_{111\phi 1}) \qquad £¨7£©$$

Where $\theta_{111z}$ and $\theta_{111\phi 1}$ were Bragg angles of $(111)_z$ and $(111)_{\phi 1}$, respectively. Integration strength was composed of structural factor, angle factor, multiplicity factor, temperature element and so on. Due to small thermal mismatch strain, with the exception of multiplicity factor, the other factors were the same both to $(111)_z$ and $(111)_{\phi 1}$. As a matter of fact, the multiplicity factor of $(111)_{\phi 1}$ was just three times than that of $(111)_z$. Therefore, Eqn.(7) can be expressed into the following again:

$$I_{111}(\theta) = c[G_{111z}(\theta - \theta_{111z}) + 3 \cdot G_{111\phi 1}(\theta - \theta_{111\phi 1})] \qquad £¨8£©$$

Where c was a constant related to structural factor, angle factor and temperature element etc. Consequently, 111 diffraction peak position ($\theta_{111}$) for the randomly oriented composites can be obtained by working out the following equation £º

$$\left( \frac{\partial G_{111z}(\theta - \theta_{111z})}{\partial \theta} + 3 \frac{\partial G_{111\phi 1}(\theta - \theta_{111\phi 1})}{\partial \theta} \right) \Bigg|_{\theta = \theta_{111}} = 0 \qquad £¨9£©$$

in which $\theta_{111}$ was the Bragg diffraction angle of 111 crystal plane. Gauss function was selected as the normalized peak shape function. In fact, it was proved that the following analysis holds for all the cases of any bell-cover shape function chosen for around the peak summit.

$$G_i(\theta) = \frac{2\sqrt{\ln 2}}{\sqrt{\pi} H_i} \exp[-\frac{4\ln 2}{H_i^2}(2\theta - 2\theta_i)^2] \qquad £¨10£©$$

where, sub. $i$ represented $(111)_z$ or $(111)_{\phi 1}$, $H_i$ was semi-height width of peak. Substitution of (10) into (9), application of the Tayloy expansion, neglecting high-order infinitesimal, so:

$$\theta_{111} - \theta_{111z} + 3\left(\frac{H_{111z}}{H_{111\phi 1}}\right)^3 (\theta_{111} - \theta_{111\phi 1}) = 0 \qquad £¨11£©$$

On the basis of the assumption of columnar whiskers, Toraya[12] method can be used to determine the width of diffraction peak. If the diameter of the whisker was D and the height was h, semi-height width H of diffraction peak and integration width $b$ will comply with the following expression:

$$H = c_1 \cdot b \qquad £¨12£©$$

Where $c_1$ was a constant related to peak shape function. Another group of equations have been founded:

$$\left.\begin{aligned} &\beta = \frac{\lambda}{h\cos\theta} \qquad \varphi = 0 \\ &\beta = \frac{\pi\sin\varphi}{D}[\frac{8}{3} + 2q\cos^{-1}q - \frac{\sin^{-1}q}{2q} - \frac{5}{2}(1-q^2)^{1/2} + \frac{1}{3}(1-q^2)^{3/2}]^{-1}\frac{\lambda}{\cos\theta} \\ &\qquad\qquad 0 < \varphi \le \chi \\ &\beta = \frac{\lambda\sin\varphi}{D}(\frac{8}{3} - \frac{\pi D}{4H}\cot\varphi)^{-1}\frac{\lambda}{\cos\theta} \qquad \chi < \varphi \le \pi/2 \end{aligned}\right\} \qquad £¨13£©$$

where $\theta$ was diffraction angle, $\varphi$ was the angle between the axial direction of the column and diffraction vector, $\chi$£½tan$^{-1}$($D$/$h$), $q$ = (h/D)tan$x$. When the aspect ratio of the whisker achieves 25 value, $\chi$£½2.29°. The angle between diffraction vector of $(111)_z$ and longitudinal axis of the whisker was $\pi/2$, and that of $(111)_{\phi 1}$ was cos$^{-1}$(1/3). The average aspect ratio of the whiskers in the squeeze cast was determined to be about 25, from which the value of $\left(H_{111z}/H_{111\phi 1}\right)$ was figured out about $10^{-3}$. In the first order approximation, the second item in the left in Eqn. (11) can be neglected, as a result, $\theta_{111} = \theta_{111z}$. After differentiating two sides of the equation, combining the Bragg equation, another new formula can be obtained:

$$\varepsilon_{111} = \frac{d_{111} - d_{111}^0}{d_{111}^0} = \varepsilon_z \qquad £¨14£©$$

Here, although 111 diffraction peak for the randomly oriented composites were comprised of those of $(111)_z$ and $(111)_{\phi 1}$, compared to $(111)_z$ diffraction peak, that of $(111)_{\phi 1}$ was so seriously widening that the peak location of 111 diffraction peak still depended upon that of $(111)_z$ in the vicinity of peak summit.

Fig.3-b indicated that the <200> direction perpendicular to {200} crystal plane makes an angle of $\phi_2$ (which equal to $\pm\cos^{-1}(1/\sqrt{3})$ ) with $[111]_z$ direction. The strain obtained from 200 diffraction peak made an angle of $\phi_2$ with the longitudinal axis of the whisker. Based on elastic mechanics, the strains relationship can be established:

$$\varepsilon_{200} = \varepsilon_{\phi 2} = \cos^2 \phi_2 \varepsilon_z + \sin^2 \phi_2 \varepsilon_r = \frac{1}{3}\varepsilon_z + \frac{2}{3}\varepsilon_r \quad £¨15£©$$

In the above formula, $\varepsilon_{200}$ represented the strain obtained from 200 diffraction peak, others were the same as those mentioned previously.

{220} crystal planes can be classified into two groups: one included six crystal planes labelled $(220)_r$ that were all perpendicular to the longitudinal axis direction of the whisker. The other was referred to as six crystal planes were denoted as $(220)_{\phi 3}$ which made the angle of $\phi_3 = \pm\cos^{-1}(\sqrt{2/3})$ with the longitudinal axis of the whisker as shown in Fig. 3-c.

Similar to formula (11), as for two groups of {220}, the following relationship worked:

$$\theta_{220} - \theta_{220r} + \left(\frac{H_{220r}}{H_{220\phi 3}}\right)^3 (\theta_{220} - \theta_{220\phi 3}) = 0 \quad £¨16£©$$

It was worth noting that the multiplicity factor of $(220)_r$ were the same as that of $(220)_{\phi 3}$. Therefore, the second item in Eqn. (16) can not introduce the constant 3 compared to Eqn. (11). According to Eqn. (13) to take the aspect ratio of the whisker as 25, a new equation can be obtained:

$$\theta_{220} = \frac{5}{6}\theta_{220\phi 3} + \frac{1}{6}\theta_{220r} \quad £¨17£©$$

Different two sides of the above expression and combine with the Bragg equation, the above equation can be turned as the following:

$$\varepsilon_{220} = \frac{5}{6}\varepsilon_{220\phi 3} + \frac{1}{6}\varepsilon_{220r} \quad £¨18£©$$

In terms of elastic mechanics, Eqn. (18) can be again rewritten as the following expression:

$$\varepsilon_{220} = \frac{5}{9}\varepsilon_z + \frac{4}{9}\varepsilon_r \quad £¨19£©$$

Theoretically, $\varepsilon_{111}$, $\varepsilon_{200}$, $\varepsilon_{220}$ can be determined. So strain components $\varepsilon_z$, $\varepsilon_r$ of the whisker can also be calculated. Furthermore, according to Eqn.(1), radial and longitudinal components of residual thermal mismatch stress in the whisker can easily be obtained.

In addition, balance equation (6) of thermal mismatch stresses was applied to calculate phase average residual stress in the matrix.

## MEASUREMENT OF THERMAL MISMATCH STRAINS

Measurement accuracy of thermal mismatch strain in the SiC whisker was conditioned by diffraction angle measurement by means of X-ray diffraction. Given that diffraction angles of 111, 200, 220 crystal planes were comparatively low, a great error may be incorporated using the common measurement method. However, in the case of high angle diffraction of the whisker, the relationship between diffraction peak displacement and strain components in the whisker was quite complex, what is more, diffraction strength of high angle diffraction peak was weak due to 20~30% volume fraction of the whiskers, which can also cause error on locating the peak. So 111, 200, 220 diffraction peaks were preferentially chosen for measuring.

The commonly used scan method can be affected by many factors such as slit width, focusing condition and scan velocity etc., while a better step scan method was employed to measure diffraction peak. Separation and calculation of peaks were carried out by computer. Under the same diffraction conditions, the main error of the step scan method was zero-angle error, to minimize the error, the difference between diffraction angles was utilised to measure thermal mismatch strain in the whisker.

The difference between 200 and 220 diffraction peak can be clearly expressed by:

$$\begin{aligned}\delta_1 &= (\theta_{220} - \theta_{200}) - (\theta^0_{220} - \theta^0_{200}) = \Delta\theta_{220} - \Delta\theta_{200} \\ &= \tan\theta^0_{200}\varepsilon_{200} - \tan\theta^0_{220}\varepsilon_{220}\end{aligned} \qquad £¨20£©$$

in which the differentiation of Bragg equation had been introduced. $\theta^0_{200}$ and $\theta^0_{220}$ can be precisely determined by extrapolating free whisker powder diffraction peak or comparing with standardized specimens.

As for 220 and 111 diffraction peaks the similar relationship can also be obtained:

$$\begin{aligned}\delta_2 &= (\theta_{220} - \theta_{111}) - (\theta^0_{220} - \theta^0_{111}) = \Delta\theta_{220} - \Delta\theta_{111} \\ &= \tan\theta^0_{111}\varepsilon_{111} - \tan\theta^0_{220}\varepsilon_{220}\end{aligned} \qquad £¨21£©$$

Strains expressions can be written as the following:

$$\left.\begin{aligned}\varepsilon_z &= (6B(\delta_1 - \delta_2) + 9\delta_2 A)/(9CA - 3AB - 6BC) \\ \varepsilon_r &= (9C - 5B)(6B(\delta_1 - \delta_2) + 9\delta_2 A)/(4B(9CA - 3AB - 6BC))\end{aligned}\right\} \qquad £¨22£©$$

where A£½$\tan\theta^0_{200}$£¬B = $\tan\theta^0_{220}$£¬C = $\tan\theta^0_{111}$ . Substitution of Eqn. (22) into Eqn. (1), radial and longitudinal stresses ($\sigma_r$, $\sigma_z$) in the whisker can be achieved.

It should be pointed out that the differences between 111, 200 and 220 diffraction anglers instead of absolute values of those were employed to eliminate zero-angle error on using the step scan method.

Radial and longitudinal thermal mismatch strains, stresses in the whisker, the intrinsic phase average thermal mismatch stress in whisker and matrix in quenched SiCw/Al composite were outlined in Table.1. Residual thermal mismatch stress in the reinforcement was compressive, and that tensile in the matrix, which agreed well with previous theoretical analyses and neutron-diffraction measurement results[13,14]. It suggested that the measurement method put forward in the paper was qualitatively reasonable. From a thermal mismatch stresses in the matrix were a little lower than those for the SiCp/Al composite reported by Reference 13.

Table 1 Thermal mismatch stresses in SiC whisker and Al matrix

| SiC whisker | | | | | Al-matrix |
|---|---|---|---|---|---|
| $\varepsilon_r(10^{-4})$ | $\varepsilon_z(10^{-4})$ | $\sigma_r$, MPa | $\sigma_z$, MPa | $\sigma^0_w$, MPa | $\sigma^0_m$, MPa |
| -7.2 | -3.9 | -470 | -348 | -429 | 107 |

## CONCLUSIONS

On the basis of the above discussion and analysis, average mismatch stresses as well as radial and longitudinal stress components in the whisker were easily available by determining the displacements of high-strength and smooth 111, 200 and 220 diffraction peak, by means of the

commonly used X-ray diffraction technology, which was often beyond reach of the other well known measurement methods.

Still, it was necessary to point out that the samples used in the X-ray diffraction experiments were so thin that the effect of macroscopic residual stresses on measurement results can be neglected. However, when thick samples were investigated, interactions of several residual stresses should be seriously taken into consideration, the contents concerning which will be published in the future. Of course, readers can also refer to Doctorate thesis of Q. Y. Liu published by Harbin Institute of Technology in 1998.

## ACKNOWLEDGEMENTS

The authors are grateful to Dr. J. J. Zhu for his helpful discussion working with Institute of Mechanics, Chinese Academy of Sciences.

## REFERENCES

[1] Hong Yan Zhang, Anderson, P.M., and Daeha, G.S., "Analysis of Thermal Induced Stress in Continous Fiber - Reinforced Composite", Metall. *Mater. Trans. A*, Vol. 25A, No. 2, 1994, pp. 415-425.

[2] Davis, L.C., and Alliwon, J.E., "Residual Stresses and Their Effect on Deformation in Particle - Reinforced Metal Matrix Composite", *Metall. Trans. A*, Vol. 24A, No. 11, 1993, pp. 2487 - 2469.

[3] Arsenault, R.J., and Wu, S.B., "The strength Differential and Bauschinger Effect in SiC - Al Composite", *Mater. Sci. Eng.*, Vol. 96, 1987, pp. 77 - 81.

[4] Taya, M., and Arsenault, R.J., "Metal Matrix Composite: Thermal-Mechanical Behavior", *Pergamen Press*, 1989, pp. 101.

[5] Chun - Hway Hsueh and Paul F. Beche. "Residual Thermal Stress in Ceramic Composite, Part ¢ò With short Fiber", *Mater. Sci. Eng. A*, Vol. A212, 1996, pp. 29 - 35.

[6] Durodola, J.F., and Derby, B., "An Analysi of Thermal Residual Stress in Ti - 6Al -4V Alloy Reinforced with SiC and $Al_2O_3$", *Acta Metall. Mater.*, Vol. 42, 1994, pp. 1525 - 1543.

[7] Povirk, G.L., Stout, M.G., and Bourke, M., "Thermal and Mechanicallly Induced Residual Stress in Al - SiC Composite", *Acta Metall. Mater.*, Vol. 40, 1992, pp. 2391 - 2412.

[8] Mouritz, A.P., and Bardyopadhayay, S., "Measurements of the Bauschinger Effect in Some Particulate $Al_2O_3$/Al and SiC/Al Metal Matrix Composite", *Scripta Metall. Mater.*, Vol. 28, 1993, pp. 1353 - 1358.

[9] Povirk, G.L., Needleman, A., and Nutt, S.R., "An Analysis of the Effect of Residual Stresses on Deformation and Damage Mechanisms in Al-SiC Composites", *Mater. Sci. Eng.*, Vol. A132, 1991, pp. 31-38.

[10] Fan, X., "X-ray diffraction of Metal", *Mechanic Industry Press*, 1989, pp. 92 - 102.

[11]Geng, L., and Yao, C.K., "SiC - Al Interface Structure in Squeeze Cast SiCw/Al Composite", *Scripta Metall. Mater.*, Vol. 33, 1995, pp. 949 - 952.

[12]Ma, L.T., "New Starting of X-ray Powder Diffraction - Rietveld Whole Pattern Fitting", *Progress in Physics (China)*, Vol. 16, No. 2, 1996, pp. 251 - 271.

[13]Meada, K, and Wakashima., K., "Stress State in Quenched SiC/Al Particulate Composite Examined by Nutron Diffraction", *scripta Mater.*, Vol.36, No. 3, 1997, pp. 335 - 340.

[14] Chun, N.J., Daniel., I.M., "Residual Thermal Stresses in Filamentary SiC/Al composite", *Comp. Eng.*, Vol. 5, No. 4, 1995, pp.425-436.